

LaBaCuFeO_{5+δ}–Ce_{0.8}Sm_{0.2}O_{1.9} as composite cathode for solid oxide fuel cells

Qingjun Zhou^{*}, Wei Wang, Tong Wei, Xuelian Qi, Yan Li,
Yunling Zou, Ye Liu, Zepeng Li, Yao Wu

College of Science, Civil Aviation University of China, Tianjin 300300, PR China

Received 5 September 2011; received in revised form 17 September 2011; accepted 17 September 2011

Available online 22 September 2011

Abstract

The performance of the LaBaCuFeO_{5+δ}–Ce_{0.8}Sm_{0.2}O_{1.9} (LBCF–SDC) composite cathodes was studied in this paper. Electrical conductivity, thermal expansion and electrochemical properties were investigated by four probing DC technique, dilatometry, AC impedance and polarization techniques, respectively. The thermal expansion coefficients of the LBCF–SDC were between $(16.3 \text{ and } 13.4) \times 10^{-6} \text{ K}^{-1}$ from 30 to 850 °C, which was lower value than LBCF ($17.0 \times 10^{-6} \text{ K}^{-1}$). AC Impedance spectroscopy measurements of LBCF–SDC/SDC/LBCF–SDC test cell were carried out. Polarization resistance values for the LBCF–SDC10 cathode was as low as $0.097 \Omega \text{ cm}^2$ at 750 °C.

© 2011 Elsevier Ltd and Techna Group S.r.l. All rights reserved.

Keywords: B. Composites; C. Thermal expansion; D. Perovskites; E. Fuel cells

1. Introduction

Solid oxide fuel cell (SOFC) is all-solid electrochemical device which converts chemical energy directly into electric power with high conversion efficiency and low to zero emission [1]. Recently, the development of intermediate-temperature solid oxide fuel cells (IT-SOFCs) is considered to be a realistic approach to practical application and commercialization [2–4]. However, the electrochemical activity of the cathode dramatically decreases with decreasing temperature. At lower temperatures, the cathode becomes the limiting factor in determining the overall cell performance. Therefore, the development of new electrodes with high-electrocatalytic activity for the oxygen-reduction reaction is crucial to achieve a favorable cell performance at intermediate temperature range (600–800 °C).

Recently, a family of oxides such as LnBaCuMO_{5+δ} (Ln = rare earth, M = Co, Fe) with the layered perovskite-type structure has drawn much attention for its potential application as IT-SOFCs cathode [5–12]. The preliminary results showed that the layered perovskite structure oxides LnBaCuMO_{5+δ} are

very promising candidates as cathode materials for application in IT-SOFCs. However, to our best knowledge, when the Co occupying the B-sites, often suffer from some problems like high thermal expansion coefficients (TEC), poor stability and high cost of cobalt element. It is desirable to develop the cobalt-free cathodes with good electrocatalytic activity for IT-SOFCs. Therefore, in order to reduce disadvantages and improve the performance, much attention should be paid to cobalt-free layered perovskite cathode.

In this study, we systematically investigated the performance of LaBaCuFeO_{5+δ}. Our aim was to improve the electrochemical performance and reduce TEC mismatch between cathode and electrolyte. The LBCF–SDC composite cathodes were investigated by X-ray diffraction, electrical conductivity, thermal expansion coefficient measurements and electrochemical impedance spectroscopy technique.

2. Experimental procedures

The LaBaCuFeO_{5+δ} (LBCF) oxide was synthesized by conventional solid-state reaction methods. Stoichiometric amounts of commercial powders La₂O₃ (99.99%), BaCO₃ (99%), CuO (99%), and Fe₂O₃ (99.5%) were ground thoroughly with ethanol as grinding medium using an agate

^{*} Corresponding author. Fax: +86 022 24092514.

E-mail address: zhouqingjun2004@yahoo.com.cn (Q. Zhou).

pestle and mortar. The obtained precursors were then pressed into pellets and calcined repeatedly at 950, 970 and 1000 °C for 10 h in air with intermediate grindings, respectively. SDC powders were synthesized with the glycine–nitrate process described elsewhere [13]. The obtained LBCF powder was mixed with different amounts of SDC powder (0–50 wt%) to make composite cathodes (denoted here by “LBCF–SDC x ”, $x = 0, 10, 20, 30, 40$, and 50). These LBCF–SDC x powders were pressed into pellets followed by sintering at 950 °C for 2 h. The sintered pellets were used for the electrical conductivity and the TEC measurements. The cathode powders were mixed with ethylcellulose and terpineol to obtain well-distributed cathode slurry. LBCF–SDC x electrodes were screen-printed onto both sides of the SDC electrolytes and sintered at 950 °C for 2 h in air, respectively.

X-ray diffraction (DX-2000) was used to confirm the crystalline structure of the prepared powders. The electrical conductivities of sintered LBCF–SDC x pellets were measured using the four probing DC technique. The TEC for each LBCF–SDC x samples was measured using a Netzsch DIL 402C dilatometer, which operated in a temperature range from 30 to 850 °C with an air purge flow rate of 60 ml min⁻¹. AC impedance spectroscopy of the symmetrical cell was tested under open-circuit conditions using an electrochemical impedance spectrum analyzer (Zaher Im6ex). The frequency range was 0.1 Hz to 1 MHz with signal amplitude of 10 mV over a temperature range 650–800 °C. Morphologies of the cathode after electrochemical test were characterized by a scanning electron microscope (SEM, JSM-6480LV, JEOL, Japan).

3. Results and discussion

Fig. 1 shows the XRD patterns of 50 wt% LBCF–50 wt% SDC mixtures calcined at 950 °C for 2 h. For comparison, the patterns of LBCF and SDC powders are also shown in the same figure. After the LBCF–SDC mixture was sintered at 950 °C, LBCF and SDC retained their own structures, respectively. No reaction products were detected by XRD. It seems that LBCF cathode is chemically compatible with the SDC electrolyte for temperatures up to 950 °C for 2 h.

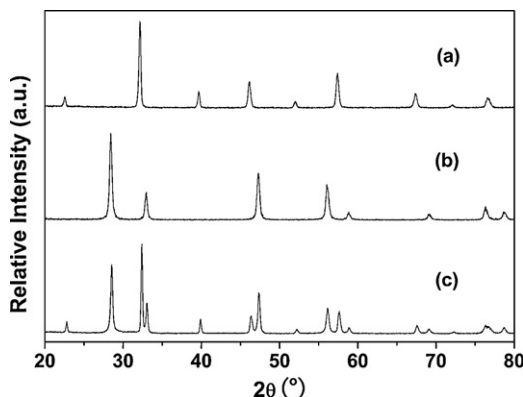


Fig. 1. X-ray diffraction patterns of (a) LBCF, (b) SDC and (c) LBCF–SDC composites sintered at 950 °C for 2h.

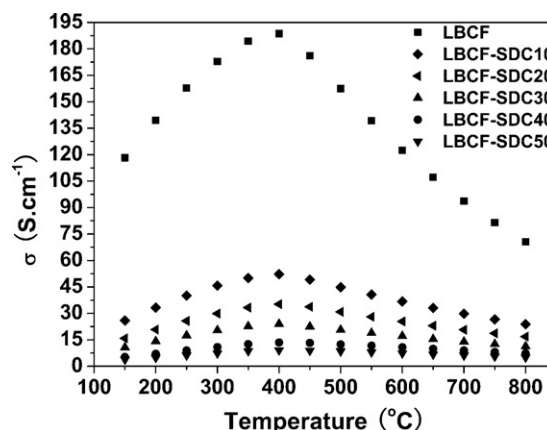


Fig. 2. Temperature dependence of the electrical conductivity of The LBCF–SDC x samples with different SDC contents in air. Conductivity data of sample LBCF were taken from Ref. [6].

Fig. 2 shows the temperature dependence of the electrical conductivities of LBCF–SDC samples with different SDC contents measured in air. It can be seen that there is an abrupt change of slope at around 400 °C, which undergoes from a semiconducting-like conduction behavior to metal-like conduction behavior. The Arrhenius plots of conductivity of LBCF–SDC x are presented in Fig. 2. As can be seen, the Arrhenius plots of conductivity are nearly linear in low temperature range (<400 °C), i.e., the conductivity (σ) dependence of temperature (T) can be expressed as

$$\sigma = \left(\frac{A}{T}\right) \exp\left(\frac{-Ea}{kT}\right) \quad (1)$$

where A is the pre-exponential constant, k is the Boltzmann constant, T is the absolute temperature, and Ea is activation energy of the electrical conductivity. By introducing SDC as the second phase, a drop in electrical conductivity was observed, where higher amounts of SDC resulted in a decrease in conductivity.

Fig. 3 shows the thermal expansion curves of LBCC–SDC x and SDC samples in the temperature range of 30–850 °C in air. Specific TEC values were presented in Table 1. As can be seen, compared with the TEC of LBCF, the TEC of LBCF–SDC

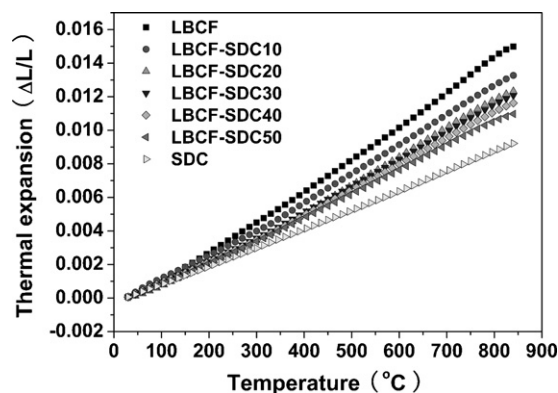


Fig. 3. Thermal expansion curves of composite cathodes in the temperature range of 30–850 °C in air.

Table 1

Average thermal expansion coefficients for LBCF–SDC_x composites and electrolyte between 30 and 850 °C in air.

Sample	TEC ($\times 10^{-6} \text{ K}^{-1}$)
LBCF	17.0
LBCF–SDC10	16.3
LBCF–SDC20	15.1
LBCF–SDC30	14.8
LBCF–SDC40	14.2
LBCF–SDC50	13.4
SDC	11.7

composites are low, with the values between $(16.3 \text{ and } 13.4) \times 10^{-6} \text{ K}^{-1}$ from 30 to 850 °C in air. It can be clearly seen that the mismatch between pure LBCF and SDC electrolyte material is large. As expected, the introduction of SDC into LBCF cathode efficiently reduces the TEC of the composite cathodes. The reduction of the TEC of composite cathode is mainly attributed to smaller TEC of SDC, for example, the TEC of SDC is $11.7 \times 10^{-6} \text{ K}^{-1}$ in the temperature range of 30–850 °C in air. The LBCF–SDC50 composite cathode provide better thermal expansion compatibility with the SDC electrolyte with a TEC value of $13.4 \times 10^{-6} \text{ K}^{-1}$ in Fig. 3. Thus, the use of a composite cathode can efficiently reduce the thermal expansion mismatch between the cathode and the electrolyte.

Fig. 4 shows the impedance spectra of the symmetrical cells using LBCF–SDC_x at 750 °C. The intercepts of the semicircle on the real axis at high-frequency region represent the total ohmic resistivity of the electrolyte and lead wire, whereas the resistance between the two intercepts with the real axis corresponds to the interfacial polarization resistances R_p . It is obvious that the addition of an ionically conducting phase SDC to LBCF cathode resulted in a significant reduction of the total interfacial polarization resistances.

Fig. 5 demonstrates the variation of R_p in the LBCF–SDC_x composite cathode with the SDC content and temperature. It is clear that R_p decreases as the temperature

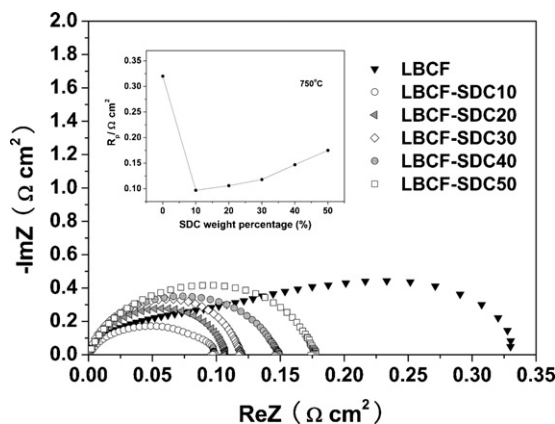


Fig. 4. Nyquist diagrams of the impedance spectroscopy for composite cathodes measured at 750 °C in air.

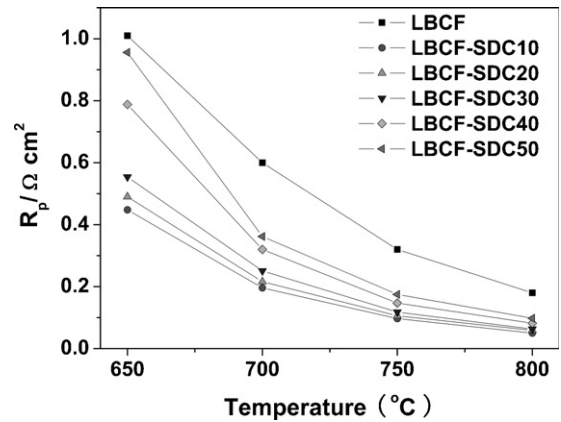


Fig. 5. Change of the polarization resistance with the SDC contents and temperature.

and SDC content increase. The R_p is the smallest when the content of SDC is 10 wt%. A further increase in SDC content results in a higher interfacial polarization resistance. This may be due to a decrease in the continuity of the LBCF phase

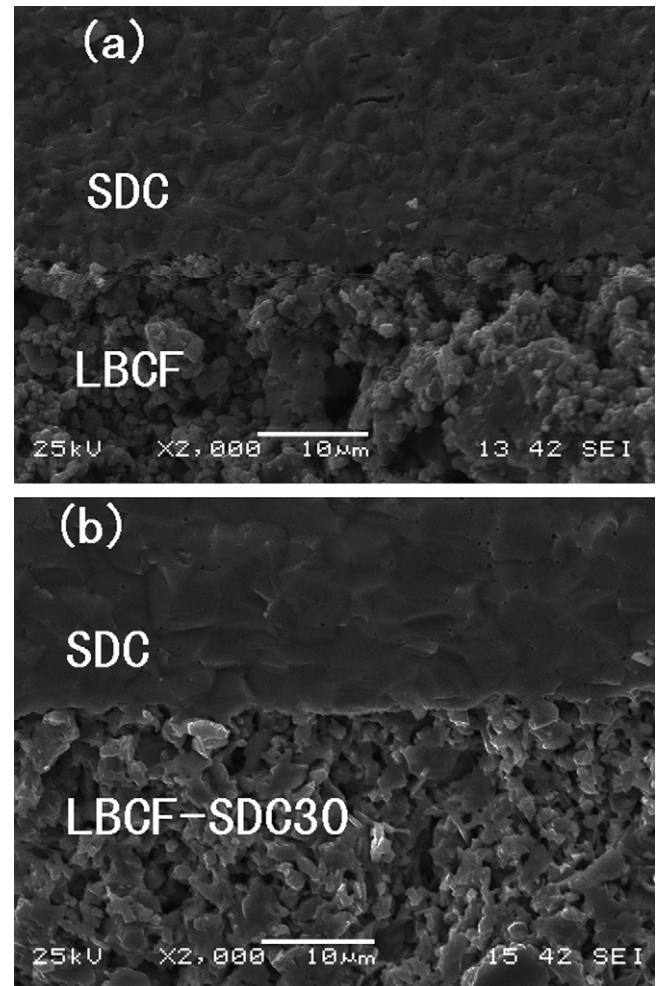


Fig. 6. SEM micrographs of (a) LBCF/SDC and (b) LBCF–SDC30/SDC interfaces.

and decrease in electrical conductivity in the composite cathodes. The non-continuous path for electronic transport may lead to the high ohmic resistance of the composite cathodes. The LBCF electrode containing 10 wt% SDC exhibits the smallest interfacial polarization resistance among the LBCF–SDC x composite cathodes, and can be explained in the following reason: the addition of high ionic conductive SDC [14] in the composite cathode, the oxygen ions transfer ability is improved and the electrochemical reaction zone is enlarged, therefore significantly improve the cathode performance. Moreover, the R_p of LBCF–SDC10 is lower than that of $\text{LaNi}_{0.6}\text{Fe}_{0.4}\text{O}_3$ – $\text{Sm}_{0.2}\text{Ce}_{0.8}\text{O}_{1.9}$, $\text{Sm}_{1.8}\text{Ce}_{0.2}\text{CuO}_4$ – $\text{Ce}_{0.9}\text{Gd}_{0.1}\text{O}_{1.95}$ and $\text{La}_{0.6}\text{Ca}_{0.4}\text{Fe}_{0.8}\text{Ni}_{0.2}\text{O}_3$ – $\text{Ce}_{0.8}\text{Sm}_{0.2}\text{O}_2$ composite cathodes [15–17].

Fig. 6 shows typical cross-SEM images of pure LBCF and LBCF–SDC30 on SDC electrolyte sintered at 950 °C for 2 h. It can be seen that the LBCF–SDC30 composite cathode has a smaller grain size and a more homogeneous grain size distribution. This means that the LBCF–SDC composite cathode layer has a finer microstructure than the pure LBCF cathode layer.

4. Conclusions

The LBCF–SDC x composite cathodes were investigated for the potential cathode for SOFCs. From the XRD results, it is found that no apparent solid-state reaction between SDC and LBCF at the temperature of 950 °C. The TEC values are reduced by mixing SDC and LBCF particles to form LBCF–SDC composite cathodes. The TEC value of LBCF–SDC50 is reduced to $13.4 \times 10^{-6} \text{ K}^{-1}$. The introduced high ion-conducting SDC electrolyte remarkably enhanced the cathode activity. The LBCF–SDC10 cathode exhibited the lowest interfacial resistance, which was about one third of pure-LBCF cathode. These results suggest that the LBCF and SDC composites are promising cathode materials for intermediate temperature SOFCs applications.

Acknowledgements

This work was supported by the Natural Science Foundation of China under contract (no. 51002183), the Scientific Research Foundation of Civil Aviation University of China (no. 09QD09X), the National Natural Science Foundation of China and the Civil Aviation Administration of China (no. 61079010), the Natural Science Foundation of China under contract (no. 51102277), and the Fundamental Research Funds for the Central Universities (no. ZXH2011D009).

References

- [1] N.Q. Minh, Ceramic Fuel Cells, *J. Am. Ceram. Soc.* 76 (1993) 563–588.
- [2] Z.P. Shao, S.M. Haile, A high-performance cathode for the next generation of solid-oxide fuel cells, *Nature* 431 (2004) 170–173.
- [3] B.C.H. Steel, A. Heinzl, Materials for fuel-cell technologies, *Nature* 414 (2001) 345–352.
- [4] C. Xia, M. Liu, Novel cathodes for low-temperature solid oxide fuel cells, *Adv. Mater.* 14 (2002) 521–523.
- [5] L. Zhao, Q. Nian, B. He, B. Lin, H. Ding, S. Wang, R. Peng, G. Meng, X. Liu, Novel layered perovskite oxide PrBaCuCoO_{5+x} as a potential cathode for intermediate-temperature solid oxide fuel cells, *J. Power Sources* 195 (2010) 453–456.
- [6] Q. Zhou, T. He, Q. He, Y. Ji, Electrochemical performances of LaBaCuFeO_{5+x} and LaBaCuCoO_{5+x} as potential cathode materials for intermediate-temperature solid oxide fuel cells, *Electrochem. Commun.* 11 (2009) 80–83.
- [7] Q. Zhou, Y. Zhang, Y. Shen, T. He, Layered perovskite GdBaCuCoO_{5+x} cathode material for intermediate-temperature solid oxide fuel cells, *J. Electrochem. Soc.* 157 (5) (2010) B628–B632.
- [8] L. Zhao, B. He, Q. Nian, Z. Xun, R. Peng, G. Meng, X. Liu, In situ drop-coated $\text{BaZr}_{0.1}\text{Ce}_{0.7}\text{Y}_{0.2}\text{O}_{3-\delta}$ electrolyte-based proton-conductor solid oxide fuel cells with a novel layered PrBaCuFeO_{5+x} cathode, *J. Power Sources* 194 (2009) 291–294.
- [9] S. Jo, P. Muralidharan, D. Kim, Enhancement of electrochemical performance and thermal compatibility of $\text{GdBaCo}_{2/3}\text{Fe}_{2/3}\text{Cu}_{2/3}\text{O}_{5+x}$ cathode on $\text{Ce}_{1.9}\text{Gd}_{0.1}\text{O}_{1.95}$ electrolyte for IT-SOFCs, *Electrochem. Commun.* 11 (2009) 2085–2088.
- [10] Y. Ling, B. Lin, L. Zhao, X. Zhang, J. Yu, R. Peng, G. Meng, X. Liu, Layered perovskite LaBaCuMO_{5+x} ($M = \text{Fe}, \text{Co}$) cathodes for intermediate-temperature protonic ceramic membrane fuel cells, *J. Alloys Compd.* 493 (2010) 252–255.
- [11] S. Lü, G. Long, Y. Ji, X. Meng, H. Zhao, C. Sun, SmBaCuCoO_{5+x} as cathode material based on GDC electrolyte for intermediate-temperature solid oxide fuel cells, *J. Alloys Compd.* 509 (2011) 2824–2828.
- [12] Z. Zhu, Z. Tao, L. Bi, W. Liu, Investigation of $\text{SmBaCuCoO}_{5+\delta}$ double-perovskite as cathode for proton-conducting solid oxide fuel cells, *Mater. Res. Bull.* 45 (2010) 1771–1774.
- [13] L. Cong, T. He, Y. Ji, P. Guan, Y. Huang, W. Su, Synthesis and characterization of IT-electrolyte with perovskite structure $\text{La}_{0.8}\text{Sr}_{0.2}\text{Ga}_{0.85}\text{Mg}_{0.15}\text{O}_{3-\delta}$ by glycine–nitrate combustion method, *J. Alloys Compd.* 348 (2003) 325–331.
- [14] G. Balazs, R. Glass, ac impedance studies of rare earth oxide doped ceria, *Solid State Ionics* 76 (1995) 155–162.
- [15] S. Huang, S. Feng, H. Wang, Y. Li, C. Wang, $\text{LaNi}_{0.6}\text{Fe}_{0.4}\text{O}_3$ – $\text{Ce}_{0.8}\text{Sm}_{0.2}\text{O}_{1.9}$ –Ag composite cathode for intermediate temperature solid oxide fuel cells, *Int. J. Hydrogen Energy* 36 (2011) 10968–10974.
- [16] L. Sun, H. Zhao, Q. Li, L. Huo, J. Viricelle, C. Pijolat, Study on $\text{Sm}_{1.8}\text{Ce}_{0.2}\text{CuO}_4$ – $\text{Ce}_{0.9}\text{Gd}_{0.1}\text{O}_{1.95}$ composite cathode materials for intermediate temperature solid oxide fuel cell, *Int. J. Hydrogen Energy* (2011), doi:10.1016/j.ijhydene.2011.07.001.
- [17] N. Ortiz-Vitoriano, I. Ruiz de Larramendi, J. Ruiz de Larramendi, M. Arriortua, T. Rojo, Optimization of $\text{La}_{0.6}\text{Ca}_{0.4}\text{Fe}_{0.8}\text{Ni}_{0.2}\text{O}_3$ – $\text{Ce}_{0.8}\text{Sm}_{0.2}\text{O}_2$ composite cathodes for intermediate-temperature solid oxide fuel cells, *J. Power Sources* 196 (2011) 4332–4336.